J. Phys. IV France **11** (2001)

Structure of melt spun $Ni_{25}Ti_{50}Cu_{25}$ ribbons studied by X-ray diffraction

T. Goryczka, M. Karolus, P. Ochin[1] and H. Morawiec

Institute of Physics and Chemistry of Metals, University of Silesia, Bankowa 12, 40-07 Katowice, Poland
[1] *CECN, CNRS, 94497 Vitry-sur-Seine, France*

ABSTRACT. Structure and transformation behaviour in NiTiCu melt spun ribbons has been investigated. The structures of amorphous and heat-treated ribbons were fitted using Rietveld refinement. After crystallisation, the following transformation sequence: B2->B19+B19' was found. The fractions of B19 and B19' phases in a mixture is equal 84 wt% 16 wt%, respectively. Quenching and annealing causes shifts in characteristic temperatures. The precipitation process is mainly responsible for the changes in the transformation course.

1. INTRODUCTION

Copper, as a ternary additional element, substituted for Ni in near equiatomic NiTi alloys, has been known to affect their transformation behaviour and shape memory characteristics. There are many ways to influence the alloy shape memory properties, where one of them is the fabrication process and/or heat treatment. New properties of ribbons are expected for non-conventional production technique – melt spinning. High quenching rate allows to obtain ribbons with unusual structure: amorphous or fine grain size. The purpose of this work was to examine structure of rapidly quenched NiTiCu alloys in amorphous and after-crystallisation states.

2. EXPERIMENTAL PROCEDURE

The bulk material with nominal composition Ni 25at.%, Ti 50 at.% and Cu 25 at.% was induction melted under helium gas atmosphere. The thin ribbons were prepared by melt spinning with an ejection pressure of 0.02 MPa onto a steel wheel rotating with the speed of 19 m/s. The obtained ribbons were 10 mm width and 46 μm thick, and showed good quality and ductility.

The transformation behaviour and the transformation temperatures were determined by Differential Scanning Calorimetery (Perkin-Elmer instrument) with cooling/heating rate of 10 K/min over the temperature range -100^0C to $+100^0$C. The X-ray diffraction pattern of an amorphous sample were obtained on Philips PW1130 diffractometer, using step-scanning mode in the 2θ range of $10\text{-}140^0$ and the graphite monochromator on the diffracted beam and molybdenum radiation (K_α Mo λ = 0.70926 [Å]). The phase identification of the alloy was established using the X-ray phase analysis on the INEL diffractometer, equipped with curved position sensitive detector CPS 120, Ge flat monochromator and temperature attachment [1]. Temperature attachment gives possibility to register X-ray diffraction patterns in temperature range between -100^0C and $+100^0$C, using the Cu $K_{\alpha 1}$ radiation with λ=1.5405[Å]. The microstructure observations were performed on thin foils using JEM3010 transmission microscope at 300kV.

3. RESULTS AND DISCUSSION

The as-spun ribbons consist of an amorphous phase, which doesn't exhibit martensitic transformation. Basing on the diffusion scattering measurements the Radial Distribution Function was calculated and tested. The radii of coordination spheres determined for nominal composition, obtained by the RDF procedure, were applied for calculation a hypothetical model of the amorphous phase in the Rietveld refinement. In case of amorphous materials the refinement was modified as performed in [2,3,4]. The results of the RDF calculation are shown in the table 1.

Table 1. The radii of coordination spheres for $Ti_{50}Ni_{25}Cu_{25}$ alloy.

	r_1	r_2	r_3	r_4	r_5	r_6	r_7
Radii [Å]	2.853	3.274	3.532	3.844	4.387	4.876	5.528

The Rietveld procedure was tested for typical model structures of *Ni-Ti* compounds: *B2, B19', R-phase, B19* and combination of them. The values of atomic radii (Ni=1.24, Ti=1.48, Cu=1.27 [*Å*]) and the compound composition (in the comparison to the initial equiatomic compound: $Ni_{50}Ti_{50}$) suggest that *Cu* atoms occupy the positions typical for *Ni* atoms. The initial results of the Rietveld refinement are shown in the table 2.

Table 2: The results of the Rietveld Refinement obtained for $Ti_{50}Ni_{25}Cu_{25}$ alloy basing on the typical model structures for *Ni-Ti* compounds.

Structure	Space group	Lattice parameters [Å]	Rwp [%]	Rp [%]
B 19'	P 1 1 21/m	a = 2.885 b = 4.622 c = 4.120 γ = 96.80	14.16	15.82
B 2	P m 3 m	a = 3.014 b = 3.014 c = 3.014	13.05	16.30
R-phase	P 3	a = 7.353 b = 7.353 c = 5.292 γ = 120.00	* * *	* * *
B 19	P21/m 2/m 2/a	a = 4.514 b = 4.279 c = 2.881	13.52	16.73
B 19' + B 2			* * *	* * *
B 19' + R			* * *	* * *

„***" – means: the values of R_{wp} are over 60 %.

Finally, the model of *B19* structure was chosen to the final Rietveld procedure. In order to increase the accuracy of the analysis, the refinement was carried out in two ranges: a first maximum of intensity (10-25° 2θ) and a second maximum (25-50° 2θ). The results are shown in the table 3 and figure 1.

Table 3. The results of the Rietveld Refinement for the structure model of B19.

Lattice parameters [Å]	Rwp [%]	Rp [%]	S [%]	Atom	Atom position	Position Occupation Parameters (POP)
first maximum (10.0 - 25.0 ° 2θ)						
a = 5.305 b = 5.040 c = 3.086	8.06	6.09	2.87	Ni Cu	x = 0.25 y = 0.50 z = 0.81	0.03 -0.96
Second maximum (25.0 - 40.0 ° 2θ)						
a = 5.770 b = 3.940 c = 2.360	6.85	5.30	1.65	Ni Cu	x = 0.25 y = 0.50 z = 0.81	0.359 -0.35

The final results of the Rietveld Refinement show that the model of *B19* unit cell was modified in the following way: a change of unit cell parameters and replacement Ni atoms by Cu atoms (x=0.25, y=0.50, z=0.81). Moreover, the Rietveld Refinement for the first and the second maximum shows two kind of structure deformation: first – relatively equally rise of unit cell parameters in a range of: a and $b \approx + 0.8$, $c \approx + 0.2$ [*Å*] and quite high values of *POP* for Cu atoms: $POP_{Cu} = 0.96$; second – not regular changes of unit cell parameters in a range of: $a \approx + 1.2$, $b \approx - 0.3$, $c \approx - 0.5$ [*Å*], which give comparable values of *POP* for *Ni, Cu* atoms and „holes": $POP \approx 0.3$.

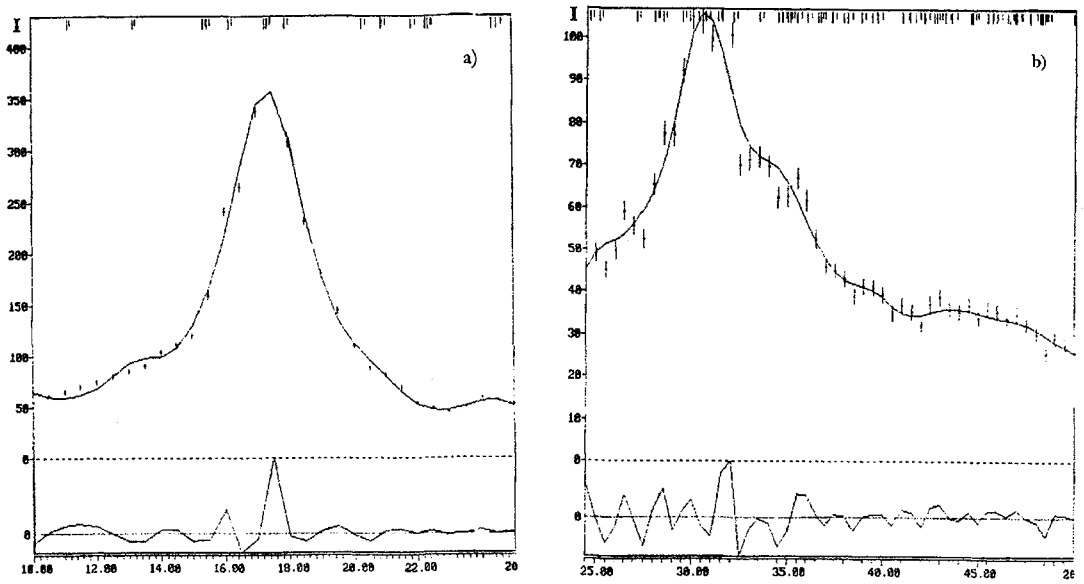

Figure 1: .The results of the Rietveld Refinement for structure model of *B19 a)* for the first maximum (10-25 2θ),b) for the second maximum (25-50 2θ).

As it has been found in [5], the melt spun ribbons undergo crystallisation at 500^{0}C. For that purpose, the studied amorphous ribbons were annealed at 600^{0}C for 1 hour. In order to study the ageing process the ribbons were quenched from 850^{0}C and additionally annealed at 700^{0}C for 30 minutes. Figure 2 shows evolution of DSC curves after thermal treatment. The solid lines indicate the transformation upon cooling, whereas the dotted lines represent reversible transformation upon heating. Table 4 contains the characteristic temperatures and thermal treatment conditions. The transformation hysteresis was evaluated as: $\Delta T = M_p - A_p$.

Table 4: The characteristic transformation temperatures for ribbons after different thermal treatment.

Sample	Thermal treatment	M_s [^{0}C]	M_f [^{0}C]	ΔH [J/g]	A_s [^{0}C]	A_f [^{0}C]	ΔH [J/g]	ΔT [^{0}C]
Bulk		61	51	13.6	5	18	13.4	
Ribbon	600 [^{0}C] /1h	65.4	46.2	11.57	61.4	74.6	11.25	11.4
Ribbon	Quenched from 850 [^{0}C]	24.1	9.2	12.8	20.2	30.7	12.3	7.6
Ribbon	Quenched from 850 [^{0}C] Annealed 700 [^{0}C] /30'	59.2	46.6	14.52	57.6	70.1	14.39	14.9

The DSC curves of crystallised ribbon exhibit sharper, higher, two overlapping peaks, which are clearly visible during both cooling and heating. It is very well known that the transformation sequence of TiNiCu shape memory alloys depends on copper content: when copper content is lower than 5at.% the transformation occurs in one step B2↔B19', when it is higher than 7.5 at.%, the two stage transformation is observed B2↔B19↔B19'. The first peak upon cooling corresponds to B2↔B19 transformation, whereas the second one to B19↔B19'. Enthalpy of the first step transformation is almost ten times higher than for the second stage. It suggests that, during temperature lowering, not all regions of B19 martensite were transformed to B19' and mixture of both martensites still exists.

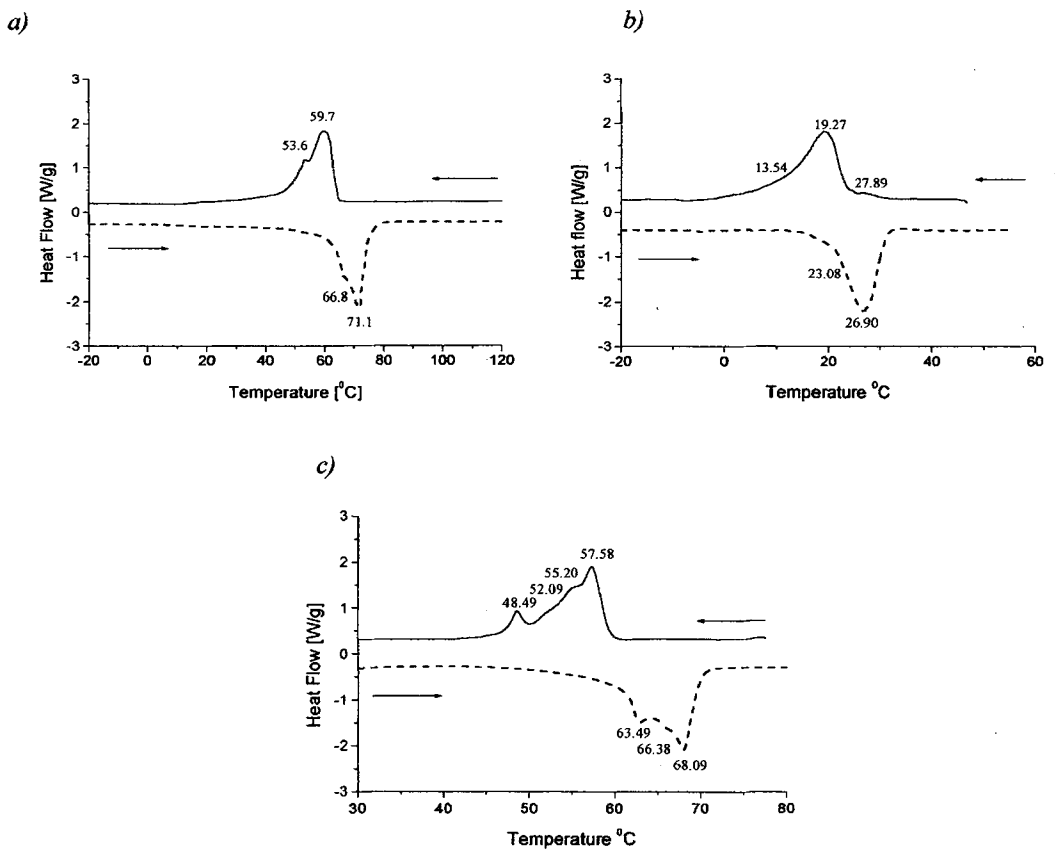

Figure 2: *Evolution of DSC curves after: a) crystallisation at 600°C/1h b) quenching from 850°C and c) quenching form 850°C and annealed 700°C/30'*

In order to determine a crystal structure and to estimate the amount of the different martensites, X-ray diffraction analysis was carried out. The DSC data show that the two-stage transformation was completed at room temperature where the X-ray diffraction pattern was taken. Quantitative phase analysis was performed with Rietveld refinement. The estimated amounts of martensites were: 86 wt.% of B19 and 14 wt.% of B19'. The reliability factors were as follows: R_p = 4.71% and R_{wp}=6.56%. Table 5 shows the final structural parameters.

Table 5: Structural parameter obtained from Rietveld Refinement for B19 and B19' martensite.

Orthorhombic martensite B19				Monoclinic martensite B19'			
Atom positions							
Element	*x*	*y*	*z*	Element	*x*	*y*	*z*
Ni	0.25	0.5	0.78320	Ni	0.01575	0.04477	0.25
Ti	0.25	0	0.29836	Ti	0.40453	0.70928	0.25
Lattice parameters [Å]							
a_0	b_0	c_0		a_0	b_0	c_0	γ
2.91880	4.28280	4.5309		2.91660	4.32490	4.41990	95.6

The goodness of fitting procedure is presented on figure 3, where crosses indicate the measured data, whereas solid line represents the calculated X-ray pattern.

After quenching, the DSC curves show irregular, broaden peak, which correspond to B2↔B19 transformation. In order to clarify the course of the phase transformation, the X-ray measurements were carried out at temperature region between +50^{0}C and -25^{0}C (fig.4). The intensity of B2 phase reflections started to decrease at 27^{0}C and weak reflections of the B19 and B19' appeared. This indicates that the M_S temperatures of B19 and B19' phases are very close and it is very difficult to distinguish them on the DSC curves. At 0^{0}C the transformation is completed. It is worth to note that, while the intensity of B19'

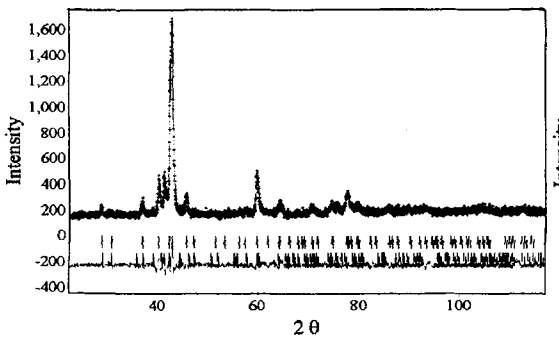

Figure 3: Rietveld Refinement result for crystallised ribbon

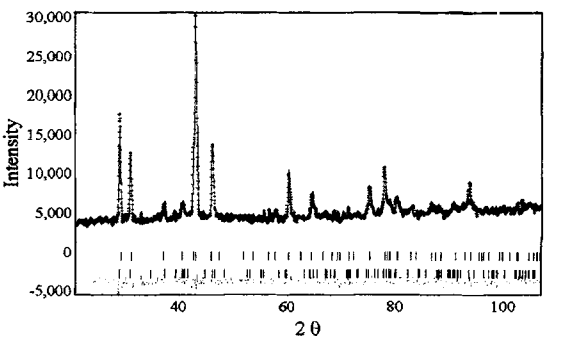

Figure 5: Rietveld Refinement results for quenched ribbon

peaks slightly increase with temperature lowering, the intensity of B19 reflections do not. X-ray quantitative phase analysis, which was carried out from the X-ray pattern (fig. 5) registered at -24^{0}C, shows that the sample contained 74 wt.% of B19 and 26 wt.% of B19' the carried out TEM observation confirmed that mainly B19 martensite was present.

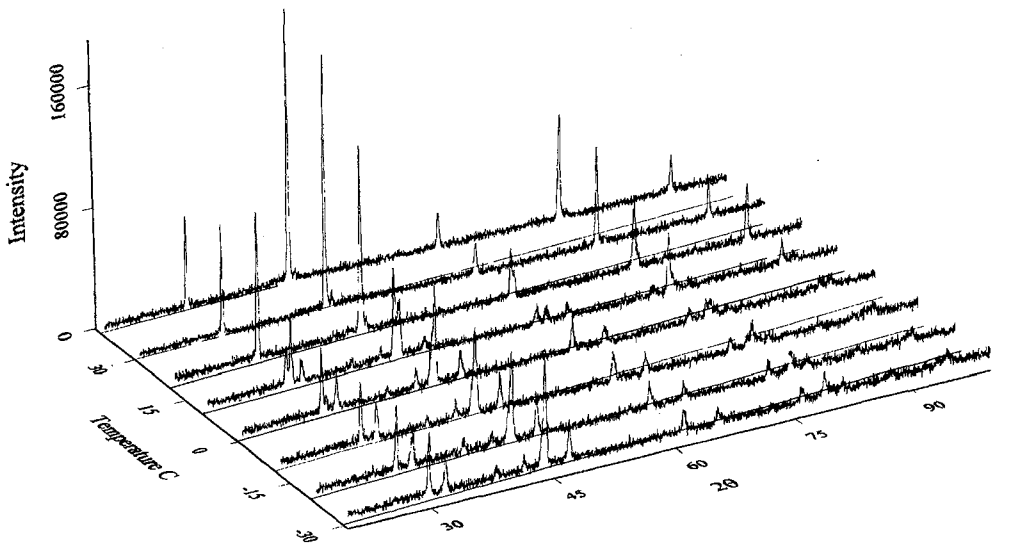

Figure 4: X-ray patterns registered upon cooling for different temperatures for quenched ribbons

In comparison to as-quenched samples, annealing at 700^{0}C for 1 hour shifts the characteristic temperatures up to 57^{0}C (M_p) and A_p -68^{0}C and splits the DSC peaks on cooling and heating curves as well. The transformation hysteresis is substantially broader. In order to explain the occurrence of additional peak on the DSC curve, the transmission electron microscopy studies were carried out. Changes of the alloy structure with different thermal treatment are shown on figure 6. Annealing at 700^{0}C causes partial recrystallisation and precipitation process. The dislocations observed in the as-quench ribbon progressively annihilate during ageing. On the other hand, the precipitates grow, especially these located at the low-angle boundaries. Two kinds of precipitates were found: small $(Cu,Ni)_3Ti_4$ and large $Ni_2Ti_5Cu_4$. Some of $(Cu,Ni)_3Ti_4$ precipitates grow inside the martensite twins (fig. 6b). The occurred precipitation process has great influence on course of the martensitic transformation, where regions with high density of precipitates have to be overcooled or overheated, depending on cooling/heating direction, respectively. Thus one can conclude that the specific arrangements of precipitates are responsible for the split in the DSC peaks.

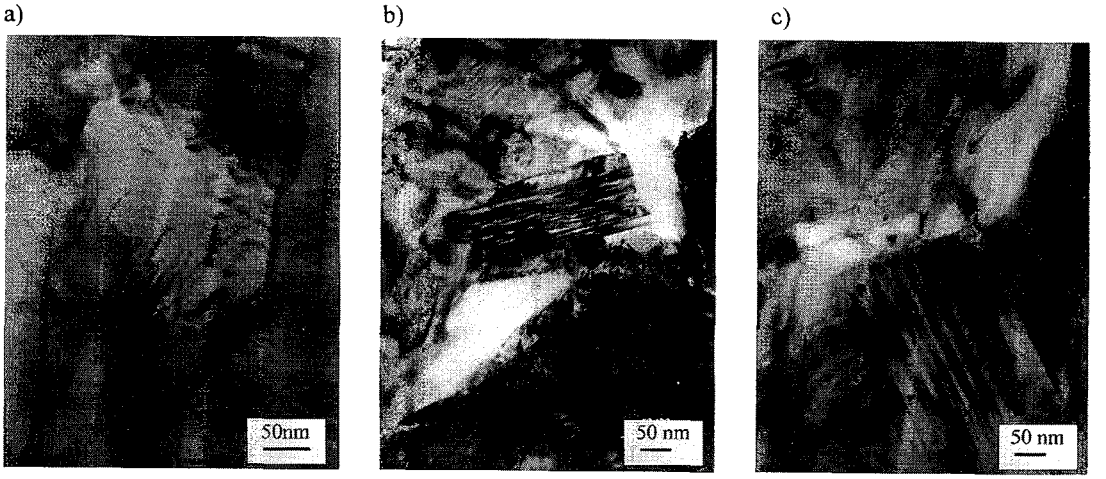

Figure 6: TEM images for: a) quenched ribbons, b) and c) annealed at 700^{0}C for 1hour

4. CONCLUSIONS

1. The refined structure of amorphous ribbons may be described as declination of atoms configuration from "equilibrium" state that corresponds to B19 martensite.
2. After crystallisation, at 600^{0}C for 1 hour, the transformation sequence B2->B19+B19' was found.
3. High temperature annealing causes formation of two kinds of precipitates: $(Cu,Ni)_3Ti_4$ and $Ni_2Ti_5Cu_4$, which shifts the transformation temperatures and broadens the transformation hysteresis.

References

[1] H. Morawiec, T. Goryczka and A. Chrobak. Mat. Sci. ForumVols. 166-169, (1994), 147.
[2] H. Krztoń, M.Niewiara - Physica Scripta **5** (1995) 98 - 101.
[3] H. Krztoń, M.Niewiara - *Proceedings of the XVI Conference on Applied Crystallography*, Cieszyn 1994, 403 - 408.
[4] M. Niewiara, E.Łągiewka - - *Proceedings of the XVII Conference on Applied Crystallography*, Wisła 1997, 156 - 159.
[5] Z.L. Xie, J. Van Humbeeck. Y. Liu and L. Delay, Scripta Mat, Vol. 37, No. 3, 1997, p363.